

# Strange and charm quark contributions to the anomalous magnetic moment of the muon

Bipasha Chakraborty,<sup>1</sup> C. T. H. Davies,<sup>1,\*</sup> G. C. Donald,<sup>2</sup> R. J. Dowdall,<sup>3</sup> J. Koponen,<sup>1</sup> and G. P. Lepage<sup>4,3</sup>  
(HPQCD collaboration),<sup>†</sup>

T. Teubner<sup>5</sup>

<sup>1</sup>*SUPA, School of Physics and Astronomy, University of Glasgow, Glasgow, G12 8QQ, UK*

<sup>2</sup>*Institut für Theoretische Physik, Universität Regensburg, 93040 Regensburg, Germany*

<sup>3</sup>*DAMTP, University of Cambridge, Wilberforce Road, Cambridge, CB3 0WA, UK*

<sup>4</sup>*Laboratory for Elementary-Particle Physics, Cornell University, Ithaca, New York 14853, USA*

<sup>5</sup>*Department of Mathematical Sciences, University of Liverpool, Liverpool, L69 3BX, UK*  
(Dated: June 3, 2014)

We describe a new technique to determine the contribution to the anomalous magnetic moment of the muon coming from the hadronic vacuum polarization using lattice QCD. Our method reconstructs the Adler function, using Padé approximants, from its derivatives at  $q^2 = 0$  obtained simply and accurately from time-moments of the vector current-current correlator at zero spatial momentum. We test the method using strange quark correlators on large-volume gluon field configurations that include the effect of up and down (at physical masses), strange and charm quarks in the sea at multiple values of the lattice spacing and multiple volumes and show that 1% accuracy is achievable. For the charm quark contributions we use our previously determined moments with up, down and strange quarks in the sea on very fine lattices. We find the (connected) contribution to the anomalous moment from the strange quark vacuum polarization to be  $a_\mu^s = 53.41(59) \times 10^{-10}$ , and from charm to be  $a_\mu^c = 14.42(39) \times 10^{-10}$ . These are in good agreement with flavour-separated results from non-lattice methods, given caveats about the comparison. The extension of our method to the light quark contribution and to that from the quark-line disconnected diagram is straightforward.

## I. INTRODUCTION

The magnetic moment of the muon can be determined extremely accurately in experiment. Its anomaly, defined as the fractional difference of its gyromagnetic ratio from the naive value of 2 ( $a_\mu = (g - 2)/2$ ) is known to 0.5 ppm [1]. The anomaly arises from muon interactions with a cloud of virtual particles. However, the theoretical cal-

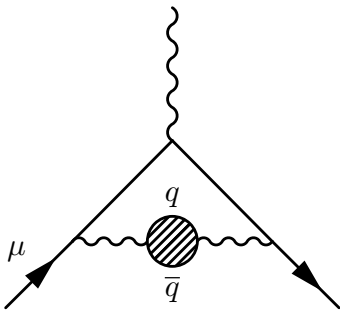


FIG. 1: The hadronic vacuum polarization contribution to the muon anomalous magnetic moment is represented as a shaded blob inserted into the photon propagator (represented by a wavy line) that corrects the point-like photon-muon coupling at the top of the diagram.

ulation of  $a_\mu$  in the Standard Model shows a discrepancy with the experimental result of about  $25(9) \times 10^{-10}$  [2–4] which could be an exciting indication of the existence of new virtual particles. Improvements of a factor of 4 in the experimental uncertainty are expected and improvements in the theoretical determination would make the discrepancy (if it remains) really compelling [5].

The current theoretical uncertainty is dominated by that from the hadronic vacuum polarization (HVP) contribution, depicted in Fig. 1. This contribution is currently determined most accurately from experimental results on  $e^+e^- \rightarrow \text{hadrons}$  or from  $\tau$  decay to be of size  $700 \times 10^{-10}$  with a 1% error [3, 4]. Higher order contributions from QCD processes, such as the hadronic light-by-light diagram, have larger percentage uncertainty but make an order of magnitude smaller contribution, so do not contribute as much to the overall theoretical uncertainty.

In 2002 Blum [6] showed how to express the HVP contribution in terms of the vacuum polarization function evaluated at Euclidean  $q^2$ , which greatly facilitates its calculation from lattice QCD. He reviews the status of such calculations in [7], which now include sea quarks [8–11]. Lattice QCD calculations, however, are not yet at a level where they can compete with the precision of values that use experimental results. A key problem has been that of determining the hadron vacuum polarization at small values of the (Euclidean) squared 4-momentum,  $q^2$ , of  $\mathcal{O}(m_\mu^2)$  which are the key ones contributing to  $a_\mu$ . Extrapolating from higher values of  $q^2$  leads to model uncertainties and direct calculation at lower  $q^2$  using ‘twisted

\*christine.davies@glasgow.ac.uk

<sup>†</sup>URL: <http://www.physics.gla.ac.uk/HPQCD>

boundary conditions' produces noisy results. Efforts are underway to improve both of these approaches [12, 13]. See also [14–16].

Here we sidestep this issue by expressing the  $g-2$  HVP contribution in terms of a small number of derivatives of the hadronic vacuum polarization function evaluated at  $q^2 = 0$ . In effect, we work upwards from  $q^2 = 0$  into the region of important, but still very small,  $q^2$  values. The advantage of this method is that the derivatives are readily and accurately computed from time-moments of the current-current correlator at zero spatial momentum.

We can approximate the hadronic vacuum polarization function by its Taylor expansion when  $q^2$  is of order  $m_\mu^2$ , but the series diverges when  $q$  is of order or larger than the threshold energy for real hadron production ( $2m_\pi$  for  $u/d$  quarks). Contributions from high momenta, say  $q \geq 1$  GeV, are suppressed by  $(m_\mu/q)^2$  but remain important if one desires better than 1% precision. To deal with high momenta, we replace the Taylor expansion by its Padé approximants [17]. Successive orders of Padé approximant converge to the exact vacuum polarization function for all positive (Euclidean)  $q^2$  [18, 19]. This follows from the dispersion relation for the vacuum polarization [13]. As we will show, only a few orders are needed to achieve 1% accuracy or better. The Padé approximants capture the entire contribution for all  $q^2$ , through analytic continuation from low  $q^2$  to high  $q^2$ , and so, unlike in some other approaches to HVP, we need not calculate high- $q^2$  contributions using perturbation theory (since this would constitute double-counting).

A further advantage of our approach is that it works with both local lattice approximations to the vector current, and exactly conserved but nonlocal approximations. Local approximations are easy to code and less noisy than nonlocal approximations, and so are widely used in lattice simulations. The fact that they are not exactly conserved leads to nonzero contributions to the vacuum polarization function  $\Pi^{\mu\nu}(q^2)$  at  $q^2 = 0$ , but such contributions are discarded automatically when we express  $g-2$  in terms of derivatives of  $\Pi^{\mu\nu}$ .

In this paper we illustrate our method by applying it to correlators made of  $s$  quarks, using well-tuned  $s$  quark masses on gluon field configurations that include up, down, strange and charm quarks in the sea. The sea up and down quarks have physical values, so no chiral extrapolation to the physical point is needed. We have three values of the lattice spacing, allowing good control of the extrapolation to zero lattice spacing. A study on three different volumes at one value of the lattice spacing allows us also to control finite volume effects.

We also give a result for the much smaller charm contribution, using moments determined previously by us [20, 21] on configurations covering a large range of lattice spacing values and including up, down and strange quarks in the sea.

The next section gives details of the lattice calculation and tests of our approach; we then discuss our results and give our conclusions.

## II. LATTICE CALCULATION

For the strange quark contribution to  $a_\mu$  we use the Highly Improved Staggered Quark (HISQ) action [27] for all quarks. This has small discretization errors [27–29] and is numerically very fast. We calculate HISQ  $s$  quark propagators on gluon field configurations generated by the MILC collaboration that include  $u$ ,  $d$ ,  $s$  and  $c$  quarks in the sea using the HISQ formalism [22, 23]. Details of the ensembles are given in Table I. They range in lattice spacing from 0.15 fm down to 0.09 fm with the spatial length of the lattice as large as 5.6 fm on the finest lattices. At each lattice spacing we have two values of the average  $u/d$  quark mass: one fifth the  $s$  quark mass and the physical value ( $m_s/27.5$  [30]). The tuning of the valence masses is more critical than that of the sea, so the valence and sea  $s$  masses differ slightly. We tune the valence  $s$  mass accurately using the mass of the  $\eta_s$ , a pseudoscalar pure  $s\bar{s}$  meson which does not occur in the real world. In lattice QCD, where the  $\eta_s$  can be prevented from mixing with other mesons, its properties can be very accurately determined [31]. Its mass (688.5(2.2) MeV [24]) is very sensitive to the  $s$  quark mass, making it useful for tuning. At a third value of the  $u/d$  quark mass, one tenth of the  $s$  quark mass, we have three different volumes to test for finite volume effects. These are sets 4, 5 and 7 and correspond to a lattice length in units of the  $\pi$  meson mass [24] of  $M_\pi L = 3.2$ , 4.3 and 5.4. In addition we de-tuned the valence  $s$  quark mass there by 5% (set 6) to test for tuning effects.

The  $s$  quark propagators are combined into a correlator with a local vector current at either end. The end point is summed over spatial sites on a timeslice to set the spatial momentum to zero. The source is created from a set of U(1) random numbers over a timeslice for improved statistics. The local current is not the conserved vector current for this quark action and must be normalised. We do this completely nonperturbatively by demanding that the vector form factor for this current be 1 between two equal mass mesons at rest ( $q^2 = 0$ ) [26]. The  $Z$  factors are given in Table I. They differ from 1 by at most 1% (on the 0.15 fm lattices) and vary from one lattice spacing to another by less than 0.5%. We therefore only calculate them for the  $m_l/m_s=0.2$  ensembles at each lattice spacing. At large time separations between source and sink these correlators give the mass and decay constant of the  $\phi$  meson [26]. Here we are concerned with the properties of the correlation function at the shorter times that feed into the theoretical determination of  $a_{\mu,\text{HVP}}$ .

The contribution to the muon anomalous magnetic moment from the HVP associated with a given quark flavour,  $f$ , is obtained by inserting the quark vacuum polarization into the photon propagator [6]:

$$a_{\mu,\text{HVP}}^{(f)} = \frac{\alpha}{\pi} \int_0^\infty dq^2 f(q^2) (4\pi\alpha Q_f^2) \hat{\Pi}_f(q^2) \quad (1)$$

where  $\alpha \equiv \alpha_{\text{QED}}$  and  $Q_f$  is the electric charge of quark  $f$

TABLE I: The lattice QCD gluon field configurations used here come from the MILC collaboration [22, 23].  $\beta = 10/g^2$  is the QCD gauge coupling, and  $w_0/a$  [24] gives the lattice spacing,  $a$ , in terms of the Wilson flow parameter,  $w_0$  [25]. We take  $w_0=0.1715(9)$  fm fixed from  $f_\pi$  [24].  $L$  and  $T$  give the length in the space and time directions for each lattice.  $am_\ell^{\text{sea}}, am_s^{\text{sea}}$  and  $am_c^{\text{sea}}$  are the light ( $m_\ell \equiv m_u = m_d$ ), strange, and charm sea quark masses in lattice units and  $am_s^{\text{val}}$ , the valence strange quark mass, tuned from the mass of the  $\eta_s$ ,  $aM_{\eta_s}$ .  $Z_{V,\bar{s}s}$  gives the vector current renormalization factor obtained nonperturbatively [26]. The lattice spacings are approximately 0.15 fm for sets 1–2, 0.12 fm for sets 3–8, and 0.09 fm for sets 9–10. Light sea-quark masses range from  $m_s/5$  to the physical value and lattice volumes ranging from 2.5 fm to 5.8 fm. The number of configurations is given in the final column. We used 16 time sources on each (12 on sets 1 and 2).

Set	$\beta$	$w_0/a$	$am_\ell^{\text{sea}}$	$am_s^{\text{sea}}$	$am_c^{\text{sea}}$	$am_s^{\text{val}}$	$aM_{\eta_s}$	$Z_{V,\bar{s}s}$	$L/a \times T/a$	$n_{\text{cfg}}$
1	5.80	1.1119(10)	0.01300	0.0650	0.838	0.0705	0.54024(15)	0.9887(20)	$16 \times 48$	1020
2	5.80	1.13670(50)	0.00235	0.0647	0.831	0.0678	0.526799(81)	0.9887(20)	$32 \times 48$	1000
3	6.00	1.3826(11)	0.01020	0.0509	0.635	0.0541	0.43138(12)	0.9938(17)	$24 \times 64$	526
4	6.00	1.4029(9)	0.00507	0.0507	0.628	0.0533	0.42664(9)	0.9938(17)	$24 \times 64$	1019
5	6.00	1.4029(9)	0.00507	0.0507	0.628	0.0533	0.42637(6)	0.9938(17)	$32 \times 64$	988
6	6.00	1.4029(9)	0.00507	0.0507	0.628	0.0507	0.41572(14)	0.9938(17)	$32 \times 64$	300
7	6.00	1.4029(9)	0.00507	0.0507	0.628	0.0533	0.42617(9)	0.9938(17)	$40 \times 64$	313
8	6.00	1.4149(6)	0.00184	0.0507	0.628	0.0527	0.423099(34)	0.9938(17)	$48 \times 64$	1000
9	6.30	1.8869(39)	0.00740	0.0370	0.440	0.0376	0.31384(9)	0.9944(10)	$32 \times 96$	504
10	6.30	1.9525(20)	0.00120	0.0363	0.432	0.0360	0.30480(4)	0.9944(10)	$64 \times 96$	621

in units of  $e$ . Here

$$f(q^2) \equiv \frac{m_\mu^2 q^2 A^3 (1 - q^2 A)}{1 + m_\mu^2 q^2 A^2} \quad (2)$$

where

$$A \equiv \frac{\sqrt{q^4 + 4m_\mu^2 q^2} - q^2}{2m_\mu^2 q^2}. \quad (3)$$

Note that in our calculation we have ignored quark-line-disconnected contributions to the HVP. These are suppressed by quark mass factors since they would vanish for equal mass  $u$ ,  $d$  and  $s$  quarks since  $\sum_{u,d,s} Q_f = 0$  [6].

The quark polarization tensor is the Fourier transform of the vector current-current correlator. For spatial currents at zero spatial momentum

$$\Pi^{ii}(q^2) = q^2 \Pi(q^2) = a^4 \sum_t e^{iqt} \sum_{\vec{x}} \langle j^i(\vec{x}, t) j^i(0) \rangle \quad (4)$$

with  $q$  the Euclidean energy. We need the renormalized vacuum polarization function,  $\hat{\Pi}(q^2) \equiv \Pi(q^2) - \Pi(0)$ . Time-moments of the correlator give the derivatives at  $q^2 = 0$  of  $\hat{\Pi}$  [32] (see, for example, [33, 34]):

$$\begin{aligned} G_{2n} &\equiv a^4 \sum_t \sum_{\vec{x}} t^{2n} Z_V^2 \langle j^i(\vec{x}, t) j^i(0) \rangle \\ &= (-1)^n \left. \frac{\partial^{2n}}{\partial q^{2n}} q^2 \hat{\Pi}(q^2) \right|_{q^2=0}. \end{aligned} \quad (5)$$

Here we have allowed for a renormalization factor  $Z_V$  for the lattice vector current. Note that time-moments remove any contact terms between the two currents<sup>1</sup>.  $G_{2n}$

is easily calculated from the correlators calculated in lattice QCD, remembering that time runs from 0 at the origin in both positive and negative directions to a maximum value of  $T/2$  in the centre of the lattice.

Defining

$$\hat{\Pi}(q^2) = \sum_{j=1}^{\infty} q^{2j} \Pi_j \quad (6)$$

then

$$\Pi_j = (-1)^{j+1} \frac{G_{2j+2}}{(2j+2)!}. \quad (7)$$

To evaluate the contribution to  $a_\mu$  we will replace  $\hat{\Pi}(q^2)$  with its  $[n, n]$  and  $[n, n-1]$  Padé approximants derived from the  $\Pi_j$  [17]. We perform the  $q^2$  integral numerically.

Eq. (5) is, of course, approximate when the temporal extent  $T$  of the lattice is finite. This error is exponentially suppressed, and usually negligible, because  $G(t)$  falls to zero quickly with increasing  $|t|$  ( $\leq T/2$ ) and has effectively vanished well before  $|t|$  gets to edge of the lattice at  $T/2$ . At large  $|t|$  the correlator is dominated by the lowest-energy vector state in the simulation —

$$G(t) \rightarrow a_0 \left( e^{-E_0|t|} + e^{-E_0(T-|t|)} \right) \quad (8)$$

— so that terms containing  $T$  are suppressed by a factor of  $\exp(-E_0 T/2)$ . Such terms become important for high order moments, since  $t^n G(t)$  peaks at  $t \approx n/E_0$  for large  $n$ , but they are negligible for the moments of interest

<sup>1</sup> The vector current need not be exactly conserved, provided that

it is renormalized correctly with  $Z_V$  because: a) there are no contributions from contact terms in the moments, and b) the only lattice operators that can mix with the vector current have higher dimension and so are suppressed by powers of  $a^2$ .

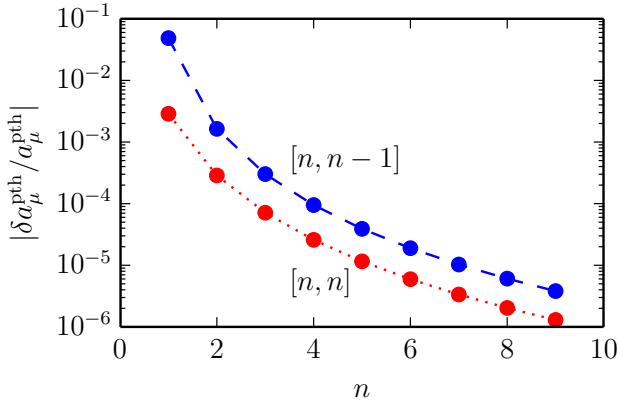


FIG. 2: Fractional error in the muon anomaly  $a_\mu$  caused by replacing the quark vacuum polarization from one-loop perturbation theory with its  $[n, n]$  and  $[n, n - 1]$  Padé approximants. The exact result is always between the  $[n, n - 1]$  and  $[n, n]$  approximants. The quark mass is set equal to the kaon mass in this test case.

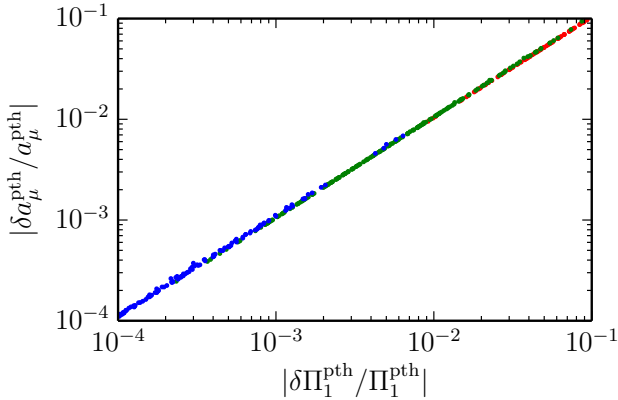


FIG. 3: Fractional errors in the muon anomaly  $a_\mu$  caused by adding random noise to the moments of the one-loop vacuum polarization. Results are shown for 400 different simulations, each with different amounts of random noise. They are plotted against the fractional uncertainty in the leading moment. In each simulation,  $[n, n]$  Padé approximants are used where  $n$  is increased until results for  $a_\mu^{\text{pth}}$  converge or spurious poles appear in the approximant. Color indicates the value of  $n$  used: red for  $[1, 1]$ , green for  $[2, 2]$ , and blue for  $[3, 3]$ . Simulation results agreed with the exact result to within  $\pm 1\sigma$  in 70% of the simulations, as expected. The quark mass is set equal to the kaon mass in each case.

here. Their impact on  $a_\mu^s$  is easily estimated (see Section III): for example, they enter at the level of 0.002% in our analysis for configuration set 10 in Table I.

The power of the Padé approximants is illustrated in Fig. 2 which shows the precision of different approximants compared with the exact result for a simple test case: the one-loop quark vacuum polarization function from perturbation theory. We set the quark mass equal to the kaon mass so that the Taylor expansion has the

same radius of convergence as the physical  $s$ -quark vacuum polarization; this function also has the same high- $q^2$  behavior as the physical function. The Padés converge exponentially quickly to the correct result, achieving better than 1% precision after only two terms are included. It is also clear that the high- $q^2$  contributions are accurately approximated by the Padés since  $q > 1 \text{ GeV}$ , for example, contributes about 1.8% of the total  $g - 2$  correction here. Note also that the  $[2, 2]$  approximant is accurate to better than 0.5% even when the quark mass is reduced to  $m_\pi$  (as one might do to simulate  $u/d$  vacuum polarization).

The results in Fig. 2 are for exact moments. The finite precision of moments from a simulation obviously limits the precision of the final results for the anomaly. The finite precision also limits the order to which Padé approximants can be computed, since noisy input data cause spurious poles to appear in high-order approximants [35]—all poles should be simple, real, and located at the poles or on the branch cut of the exact vacuum polarization function [19]. Higher orders are possible with more precise moments. The Padés typically converge before spurious poles appear, so that the precision of the final results tracks that of the input moments. This is illustrated in Fig. 3 where we have added noise to the exact moments from one-loop perturbation theory, and compare the precision of outputs with that of the inputs. Each point in the plot represents a different simulation, with different noise, and the colors indicate the order of the approximant used.

As a final check of our analysis method and our simulation codes, we generated lattice correlators using our codes but without gauge fields (that is with link variables  $U_\mu(x) = 1$ ), and verified (to 0.1%) that the results for  $a_\mu$  agree with continuum one-loop perturbation theory in the limit of zero lattice spacing.

Returning to results from our lattice simulations, the Taylor coefficients  $\Pi_j$  and contributions to  $a_\mu$  from each of our  $s$ -quark correlators are shown in Table II. In each case results converge to within errors by the  $[1, 1]$  Padé approximant, and no spurious poles appear on any of our sets up to and including  $[2, 2]$ , as expected from our test case. Our results on sets 4-7 show that finite-volume effects are negligible within our 0.1% statistical errors, but tuning the valence  $s$ -quark accurately is seen to be important.

To obtain a final estimate we fit the  $[2, 2]$  results from each configuration set to a function of the form

$$a_{\mu, \text{lat}}^s = a_\mu^s \times (1 + c_a^2 (a\Lambda_{\text{QCD}}/\pi)^2 + c_{\text{sea}} \delta x_{\text{sea}} + c_{\text{val}} \delta x_{\text{val}}) \quad (9)$$

where  $\Lambda_{\text{QCD}} = 0.5 \text{ GeV}$ , and  $\delta x_{\text{sea}}$  and  $\delta x_{\text{val}}$  allow for

TABLE II: Columns 2-5 give the Taylor coefficients  $\Pi_j$  (Eq. 6), in units of  $1/\text{GeV}^{2j}$ , for each of the lattice data sets in Table I. The errors given include statistics and the (correlated) uncertainty from setting the lattice spacing using  $w_0$ , which dominates. Estimates of the connected contribution from  $s$ -quarks to  $a_{\mu, \text{HVP}}$  are given for each of the  $[1, 0]$ ,  $[1, 1]$ ,  $[2, 1]$  and  $[2, 2]$  Padé approximants in columns 6-9; results are multiplied by  $10^{10}$ .

Set	$\Pi_1$	$\Pi_2$	$\Pi_3$	$\Pi_4$	$[1, 0] \times 10^{10}$	$[1, 1] \times 10^{10}$	$[2, 1] \times 10^{10}$	$[2, 2] \times 10^{10}$
1	0.06598(76)	-0.0516(11)	0.0450(15)	-0.0403(19)	58.11(67)	53.80(59)	53.95(59)	53.90(59)
2	0.06648(75)	-0.0523(11)	0.0458(15)	-0.0408(18)	58.55(66)	54.19(58)	54.33(59)	54.29(59)
3	0.06618(75)	-0.0523(11)	0.0466(15)	-0.0425(20)	58.28(66)	53.93(58)	54.09(58)	54.04(58)
4	0.06614(74)	-0.0523(11)	0.0467(15)	-0.0427(19)	58.25(65)	53.90(57)	54.06(58)	54.01(57)
5	0.06626(74)	-0.0527(11)	0.0473(15)	-0.0438(19)	58.36(65)	53.99(57)	54.15(57)	54.10(57)
6	0.06829(77)	-0.0557(12)	0.0514(17)	-0.0490(22)	60.14(67)	55.55(59)	55.73(59)	55.67(59)
7	0.06619(74)	-0.0524(11)	0.0468(15)	-0.0430(19)	58.29(65)	53.93(57)	54.10(57)	54.05(57)
8	0.06625(74)	-0.0526(11)	0.0470(15)	-0.0429(19)	58.34(65)	53.98(57)	54.14(57)	54.09(57)
9	0.06616(77)	-0.0531(12)	0.0483(17)	-0.0450(22)	58.27(68)	53.87(59)	54.04(60)	53.99(59)
10	0.06630(72)	-0.0534(11)	0.0487(16)	-0.0458(20)	58.39(64)	53.98(56)	54.15(56)	54.10(56)

TABLE III: Error budgets for connected contributions to the muon anomaly  $a_\mu$  from vacuum polarization of  $s$  and  $c$  quarks.

	$a_\mu^s$	$a_\mu^c$
Uncertainty in lattice spacing ( $w_0, r_1$ ):	1.0%	0.6%
Uncertainty in $Z_V$ :	0.4%	2.5%
Monte Carlo statistics:	0.1%	0.1%
$a^2 \rightarrow 0$ extrapolation:	0.1%	0.4%
QED corrections:	0.1%	0.3%
Quark mass tuning:	0.0%	0.4%
Finite lattice volume:	< 0.1%	0.0%
Padé approximants:	< 0.1%	0.0%
Total:	1.1%	2.7%

mistuning of the sea and valence light-quark bare masses:

$$\delta x_{\text{sea}} \equiv \sum_{q=u,d,s} \frac{m_q^{\text{sea}} - m_q^{\text{phys}}}{m_s^{\text{phys}}} \quad (10)$$

$$\delta x_s \equiv \frac{m_s^{\text{val}} - m_s^{\text{phys}}}{m_s^{\text{phys}}}. \quad (11)$$

For our lattices with physical  $u/d$  sea masses  $\delta x_{\text{sea}}$  is very small.  $a^2$  errors from staggered ‘taste-changing’ effects will remain and they are handled by  $c_{a^2}$ . The four fit parameters are  $a_\mu^2$ ,  $c_{a^2}$ ,  $c_{\text{sea}}$  and  $c_{\text{val}}$ ; we use the following (broad) Gaussian priors for each:

$$\begin{aligned} a_\mu^s &= 0 \pm 100 \times 10^{-10} \\ c_{a^2} &= 0(1) \quad c_{\text{sea}} = 0(1) \quad c_{\text{val}} = 0(1). \end{aligned} \quad (12)$$

Our final result for the connected contribution for  $s$  quarks to  $g - 2$  is:

$$a_\mu^s = 53.41(59) \times 10^{-10}. \quad (13)$$

The fit to  $[2, 2]$  Padé results from all 10 of our configuration sets is excellent, with a  $\chi^2$  per degree of freedom of 0.22 ( $p$ -value of 0.99). In Fig. 4 we compare our fit with the data from configurations with  $m_s/m_\ell$  equal 5 and with the physical mass ratio.

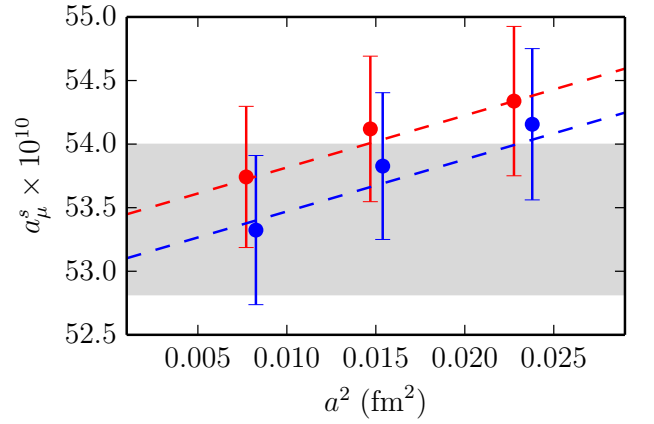


FIG. 4: Lattice QCD results for the connected contribution to the muon anomaly  $a_\mu$  from vacuum polarization of  $s$  quarks. Results are for three lattice spacings, and two light-quark masses:  $m_\ell^{\text{lat}} = m_s/5$  (lower, blue points), and  $m_\ell^{\text{lat}} = m_\ell^{\text{phys}}$  (upper, red points). The dashed lines are the corresponding values from the fit function, with the best-fit parameter values:  $c_{a^2} = 0.29(13)$ ,  $c_{\text{sea}} = -0.020(6)$  and  $c_{\text{val}} = -0.61(4)$ . The gray band shows our final result,  $53.41(59) \times 10^{-10}$ , with  $m_\ell^{\text{lat}} = m_\ell^{\text{phys}}$ , after extrapolation to  $a = 0$ .

TABLE IV: Contributions to  $a_\mu$  from  $s$  and  $c$  quark vacuum polarization. Only connected parts of the vacuum polarization are included. Results, multiplied by  $10^{10}$ , are shown for each of the Padé approximants.

Quark	$[1, 0] \times 10^{10}$	$[1, 1] \times 10^{10}$	$[2, 1] \times 10^{10}$	$[2, 2] \times 10^{10}$
$s$	57.63(67)	53.28(58)	53.46(59)	53.41(59)
$c$	14.58(39)	14.41(39)	14.42(39)	14.42(39)

The error budget for our result is given in Table III. The dominant error, by far, comes from the uncertainty in the physical value of the Wilson flow parameter  $w_0$ , which we use to set the lattice spacings. We estimate the uncertainty from QED corrections to the vacuum polar-

ization to be of order 0.1% from perturbation theory [20], suppressed by the small charge of the  $s$  quark. Our results show negligible dependence ( $< 0.1\%$ ) on the spatial size of the lattice, which we varied by a factor of two. Also the convergence of successive orders of Padé approximant indicates convergence to better than 0.1%; results from fits to different approximants are tabulated in Table IV.

Note that the  $a^2$  errors are quite small in our analysis. This is because we use the highly corrected HISQ discretization of the quark action. Our final ( $a = 0$ ) result is only 0.6% below our results from the 0.09 fm lattices (sets 9 and 10). The variation from our coarsest lattice to  $a = 0$  is only 1.8%. We compared this with results from the clover discretization for quarks, which had finite- $a$  errors in excess of 20% on the coarsest lattices.

Finally we also include results for  $c$  quarks in Tables III and IV. These are calculated from the moments (and error budget) published in [20]. Our final result for the connected contribution to the muon anomaly from  $c$ -quark vacuum polarization is:

$$a_\mu^c = 14.42(39) \times 10^{-10}. \quad (14)$$

The dominant source of error here is in the determination of the  $Z_V$  renormalization factors. This error could be substantially reduced by using the method we used for the  $s$ -quark contribution [26].

### III. DISCUSSION/CONCLUSIONS

The ultimate aim of lattice QCD calculations of  $a_{\mu, \text{HVP}}$  is to improve on results from using, for example,  $\sigma(e^+e^- \rightarrow \text{hadrons})$  that are able to achieve an uncertainty of below 1%. We are not at that stage yet. However, our results here show that a 1% error can be achieved now for the connected piece of the  $s$ -quark contribution and a 1% error could easily be achieved for the  $c$ -quark. It then makes sense to try to separate out the  $s$ -quark or  $c$ -quark piece of the result from  $\sigma_{e^+e^-}$  for comparison. The flavour identification is not completely unambiguous in that case nor can disconnected contributions or QED effects be removed, so the accuracy with which this can be done is limited.

For the  $c$ -quark contribution a result of  $14.4(1) \times 10^{-10}$  is given by [36], with which our result is in good agreement. For the  $s$ -quark contribution, we can make predictions based on the data compilation from [3] for energies up to 2 GeV in the dispersion integral and by using perturbative QCD for higher energies. The leading contribution can be estimated from the sum of the  $K^+K^-$  and  $K_L^0K_S^0$  channels, adding up to  $35.5 \times 10^{-10}$ . As most of this contribution is from the  $\phi$  resonance, we can assume that this is included in the lattice calculation. It is less clear how much of the remaining  $\phi$  decay channels should be included for the comparison, as these may require the inclusion of disconnected diagrams in the lattice calculation. However, using the branching fractions for  $\phi \rightarrow K^+K^-$  and  $\phi \rightarrow K_L^0K_S^0$  we can predict a maximum

$\phi$  contribution of  $42.8 \times 10^{-10}$ . Other channels containing  $\bar{K}K$  ( $\bar{K}Kn\pi$ ,  $\bar{K}K\omega$ ) and  $\eta\phi$ , which are taken into account in [3], add up to  $6.6 \times 10^{-10}$ . It is not clear to what extent these are included in the lattice calculation presented here and to what extent they derive from a light quark loop coupled to the electromagnetic current together with  $s$  sea quarks. The  $s$  quark contribution for energies above 2 GeV can be reliably calculated from perturbative QCD. It is  $5.9 \times 10^{-10}$  and must certainly be included in the comparison. With these numbers we predict the total  $s$  quark contribution from data and perturbative QCD to be  $55.3(8) \times 10^{-10}$ . From the caveats mentioned, this should be seen as an upper limit for the comparison with lattice QCD. Previous lattice QCD calculations have not reported separate results for  $s$  or  $c$  quarks (if calculated), despite the simplicity of doing this when only the connected contribution has been calculated. It would seem sensible to do this for comparison of different lattice results in the future.

The extension of our method for light-quark ( $u, d$ ) vacuum polarization is straightforward, with one modification. The light-quark contribution is the most important in the total HVP, being about 12 times larger than that for the strange quark, in part because of a factor of 5 from the electric charges. The one complication is that the signal-to-noise at large  $t$  is much worse for the light-quark correlators (because  $2m_\pi$  is small compared to  $m_\rho$ ), greatly increasing the statistical errors of the moments. This is easily handled by fitting Monte Carlo data for the correlator  $G(t)$  with a standard multi-exponential fit function  $G_{\text{fit}}(t, p)$ , where the  $p_\beta$  are fit parameters. The moments are then calculated from  $G_{\text{fit}}(t, p^*)$ , using the best-fit parameter values  $p = p^*$ , rather than from the data. The fit function has similar errors to the data at low  $t$ , but much smaller errors (orders of magnitude) at large  $t$ , and therefore much smaller errors in the moments. By using the fit function, we build into our  $g - 2$  analysis knowledge about how  $G(t)$ 's behavior at large  $t$  is constrained by its behavior at small  $t$ .

We tested this fitting idea on our  $s$ -quark data, using data for  $t = 0, \pm 1$  and the best-fit function ( $G_{\text{fit}}$ ) for all other  $t$  when computing moments. We obtained results identical, to four decimal places or better, with what we found above (Table II) and with slightly smaller statistical errors. We also tested this idea on a single low-statistics sample of correlators from 4 time sources on 400 configurations (a subset of Set 8 of Table I) with the valence quark mass equal to the physical light-quark mass  $m_\ell^{\text{phys}}$ . Using  $G_{\text{fit}}(t, p^*)$  in place of the  $G(t)$  reduced the statistical errors from  $\pm 100\%$  to  $\pm 6\%$ , indicating that errors of around 3% might be achieved using the full statistics. As expected the Padé approximants converged to better than 1% by the [1,1] approximant. We will discuss light quarks in a separate paper, but an uncertainty of 1%, as achieved here for  $s$  quarks, seems feasible on ensemble sizes of  $10\times$  that used here.

Using  $G_{\text{fit}}(t)$  to calculate moments also allows us to remove systematic errors caused by the finite temporal

size  $T$  of our lattices. This is because it is trivial to take  $T \rightarrow \infty$  in  $G_{\text{fit}}(t)$  after fitting but before calculating the moments. The resulting shifts in  $a_\mu$  are typically very small—for example, only 0.09% for the physical  $u/d$  quark propagators in our test analysis above—but the correction is worth making anyway because it is so simple.

Our method also provides a straightforward extension to include disconnected contributions. All that is necessary is to calculate the disconnected contribution to the vector correlator at zero spatial momentum and that can be done with existing techniques, again provided adequate statistics are available<sup>2</sup>. To reduce errors below 1% on the total HVP contribution may require direct calculation of QED effects on the lattice and the incorporation of  $u$  and  $d$  quark propagators of different mass, techniques that are being tested now in the lattice QCD community.

In conclusion, we have shown that a simple method using a small number of time-moments of vector current-current correlators can yield 1% accurate results for the

hadronic vacuum polarization contribution to  $a_\mu$ . For the connected  $s$ -quark and  $c$ -quark contributions we find, respectively,  $a_\mu^s = 53.41(59) \times 10^{-10}$  and  $a_\mu^c = 14.42(39) \times 10^{-10}$ .

*Note added.* After our paper appeared we received the results of a preliminary analysis by members of the ETM Collaboration [38], separating  $a_\mu^s$  and  $a_\mu^c$  from their analysis of the complete 4-flavour connected HVP contribution to  $a_\mu$  [39]. They find  $a_\mu^s = 53(3) \times 10^{-10}$  and  $a_\mu^c = 14.1(6) \times 10^{-10}$ , in agreement with our results.

*Acknowledgements.* We are grateful to the MILC collaboration for the use of their gauge configurations and code. We thank R. R. Horgan, G. M. von Hippel, D. Nomura, P. Rakow and D. Toussaint for useful conversations. Our calculations were done on the Darwin Supercomputer as part of STFC's DiRAC facility jointly funded by STFC, BIS and the Universities of Cambridge and Glasgow. This work was funded by STFC, the Royal Society, the Wolfson Foundation and the National Science Foundation.

- 
- [1] G. Bennett et al. (Muon G-2 Collaboration), Phys.Rev. **D73**, 072003 (2006), hep-ex/0602035.
  - [2] T. Aoyama, M. Hayakawa, T. Kinoshita, and M. Nio, Phys.Rev.Lett. **109**, 111808 (2012), 1205.5370.
  - [3] K. Hagiwara, R. Liao, A. D. Martin, D. Nomura, and T. Teubner, J.Phys. **G38**, 085003 (2011), 1105.3149.
  - [4] M. Davier, A. Hoecker, B. Malaescu, and Z. Zhang, Eur.Phys.J. **C71**, 1515 (2011), 1010.4180.
  - [5] T. Blum, A. Denig, I. Logashenko, E. de Rafael, B. Lee Roberts, et al. (2013), 1311.2198.
  - [6] T. Blum, Phys.Rev.Lett. **91**, 052001 (2003), hep-lat/0212018.
  - [7] T. Blum, M. Hayakawa, and T. Izubuchi, PoS **LAT-TICE2012**, 022 (2012), 1301.2607.
  - [8] C. Aubin and T. Blum, Phys.Rev. **D75**, 114502 (2007), hep-lat/0608011.
  - [9] P. Boyle, L. Del Debbio, E. Kerrane, and J. Zanotti, Phys.Rev. **D85**, 074504 (2012), 1107.1497.
  - [10] X. Feng, K. Jansen, M. Petschlies, and D. B. Renner, Phys.Rev.Lett. **107**, 081802 (2011), 1103.4818.
  - [11] M. Della Morte, B. Jager, A. Jüttner, and H. Wittig, JHEP **1203**, 055 (2012), 1112.2894.
  - [12] C. Aubin, T. Blum, M. Golterman, and S. Peris, Phys.Rev. **D88**, 074505 (2013), 1307.4701.
  - [13] C. Aubin, T. Blum, M. Golterman, and S. Peris, Phys.Rev. **D86**, 054509 (2012), 1205.3695.
  - [14] X. Feng, S. Hashimoto, G. Hotzel, K. Jansen, M. Petschlies, et al., Phys.Rev. **D88**, 034505 (2013), 1305.5878.
  - [15] A. Francis, B. Jaeger, H. B. Meyer, and H. Wittig, Phys.Rev. **D88**, 054502 (2013), 1306.2532.
  - [16] E. B. Gregory, Z. Fodor, C. Hoelbling, S. Krieg, L. Lelouch, et al. (2013), 1311.4446.
  - [17] The  $[m, n]$  Padé approximant of a function  $f(x)$  is a ratio of polynomials in  $x$ , of order  $m$  in the numerator and  $n$  in the denominator, whose Taylor expansion is the same as that of  $f(x)$  through order  $x^{n+m}$ .
  - [18] G. Baker, J.Math.Phys. **10**, 814 (1969), <http://dx.doi.org/10.1063/1.1664911>.
  - [19] G. Baker and P. Graves-Morris, *Padé Approximants* (Cambridge, 1996), 2nd ed., especially chapter 5.
  - [20] G. Donald, C. Davies, R. Dowdall, E. Follana, K. Hornbostel, et al. (HPQCD Collaboration), Phys.Rev. **D86**, 094501 (2012), 1208.2855.
  - [21] C. Davies, G. Donald, R. Dowdall, J. Koponen, E. Follana, et al. (HPQCD Collaboration), PoS **ConfinementX**, 288 (2012), 1301.7203.
  - [22] A. Bazavov et al. (MILC collaboration), Phys.Rev. **D82**, 074501 (2010), 1004.0342.
  - [23] A. Bazavov et al. (MILC Collaboration), Phys.Rev. **D87**, 054505 (2013), 1212.4768.
  - [24] R. Dowdall, C. Davies, G. Lepage, and C. McNeile (HPQCD Collaboration), Phys.Rev. **D88**, 074504 (2013), 1303.1670.
  - [25] S. Borsanyi, S. Durr, Z. Fodor, C. Hoelbling, S. D. Katz, et al., JHEP **1209**, 010 (2012), 1203.4469.
  - [26] B. Chakraborty, C. Davies, G. Donald, R. Dowdall, J. Koponen, et al. (HPQCD Collaboration), PoS **LAT-TICE2013**, 309 (2013), 1401.0669.
  - [27] E. Follana, Q. Mason, C. Davies, K. Hornbostel, G. P. Lepage, et al. (HPQCD and UKQCD Collaborations), Phys.Rev. **D75**, 054502 (2007), hep-lat/0610092.
  - [28] E. Follana, C. Davies, G. Lepage, and J. Shigemitsu (HPQCD and UKQCD Collaborations), Phys.Rev.Lett. **100**, 062002 (2008), 0706.1726.
  - [29] C. Davies, C. McNeile, E. Follana, G. Lepage, H. Na, et al. (HPQCD Collaboration), Phys.Rev. **D82**, 114504 (2010), 1008.4018.
  - [30] S. Durr, Z. Fodor, C. Hoelbling, S. Katz, S. Krieg, et al., Phys.Lett. **B701**, 265 (2011), 1011.2403.
  - [31] C. Davies, E. Follana, I. Kendall, G. Lepage, and C. McNeile (HPQCD Collaboration), Phys.Rev. **D81**, 034506

(2010), 0910.1229.

- [32] Eq. (5) is simply related to finite-difference approximations of derivatives of  $\hat{\Pi}(q^2)$  that use the discrete values of  $q = E_n$  allowed by the periodic  $t$ -lattice. The simplest finite-difference derivative,  $\Delta f(E_n) \equiv (f(E_{n+1}) - f(E_{n-1}))/2\delta E$  where  $\delta E = E_{n+1} - E_n$ , is accurate up to an error of order  $(\delta E)^2$ . This and higher-order errors can be removed by making successively less local approximations:

$$\Delta - (\delta E)^2 \Delta^3/6 + 3(\delta E)^4 \Delta^5/40 + \dots$$

Continuing this process to remove errors to all orders in  $(\delta E)^2$  results in the derivative defined by Eq. (5), as is evident from the Fourier transform of the improved difference operator.

- [33] I. Allison et al. (HPQCD Collaboration), Phys.Rev. **D78**, 054513 (2008), 0805.2999.  
 [34] C. McNeile, C. Davies, E. Follana, K. Hornbostel, and G. Lepage (HPQCD Collaboration), Phys.Rev. **D82**, 034512 (2010), 1004.4285.  
 [35] P. Gonnet et al., SIAM Review **55**, 101 (2013).  
 [36] S. Bodenstein, C. Dominguez, and K. Schilcher, Phys.Rev. **D85**, 014029 (2012), 1106.0427.  
 [37] M. Della Morte and A. Juttner, JHEP **1011**, 154 (2010), 1009.3783.  
 [38] G. Hotzel, K. Jansen, M. Petschlies, private communication.  
 [39] F. Burger, X. Feng, G. Hotzel, K. Jansen, M. Petschlies, et al. (2013), 1308.4327.